

Kent Academic Repository

Full text document (pdf)

Citation for published version

Taylor, P.S. and Horne, Robert and Batchelor, John C. (2018) An 8-bit UHF RFID tag for passive sensing applications. In: IET : Loughborough Antennas & Propagation Conference 2018 (LAPC 2018). . 47 -47. The Institution of Engineering and Technology, UK ISBN 978-1-78561-969-4.

DOI

<https://doi.org/10.1049/cp.2018.1468>

Link to record in KAR

<https://kar.kent.ac.uk/73797/>

Document Version

Author's Accepted Manuscript

Copyright & reuse

Content in the Kent Academic Repository is made available for research purposes. Unless otherwise stated all content is protected by copyright and in the absence of an open licence (eg Creative Commons), permissions for further reuse of content should be sought from the publisher, author or other copyright holder.

Versions of research

The version in the Kent Academic Repository may differ from the final published version.

Users are advised to check <http://kar.kent.ac.uk> for the status of the paper. **Users should always cite the published version of record.**

Enquiries

For any further enquiries regarding the licence status of this document, please contact:

researchsupport@kent.ac.uk

If you believe this document infringes copyright then please contact the KAR admin team with the take-down information provided at <http://kar.kent.ac.uk/contact.html>

An 8-bit UHF RFID tag for passive sensing applications

P.S. Taylor, R.J. Horne, J.C. Batchelor

*School of Engineering, The University of Kent, Canterbury, UK.
p.taylor-250@kent.ac.uk*

Keywords: RFID tag, passive sensing, UHF.

Abstract

This paper presents a passive UHF RFID tag consisting of a single dipole antenna matched to multiple RFID devices, where each is programmed with a unique binary weighting in its EPC register. With each device having its own digital input this results in a single tag capable of binary counting or a tag with multiple inputs. Measurement results and associated reader software demonstrate a proof of concept for an 8-bit version of the tag.

1 Introduction

Although intended for general inventory management UHF RFID has grown and seen applications beyond this, where chip and antenna designs have incorporated sensing technologies [1-5]. Some designs, although innovative may not be particularly practical and can rely on functionality not available in standard UHF readers. Offering potential in passive RFID sensing technologies presented here is a single antenna 8-bit tag design that uses standard commercial devices and reader. The tag can be used as an 8-bit counter or provide eight digital inputs for other sensing functions, all wirelessly and battery free.

2 Theory of operation

The SL3S1213 (G2IL+) [6] from NXP is a UHF Gen 2 RFID transponder IC offering several features beyond just a general inventory type device. Of interest here is its integrated tag tamper alarm, whose main function is as a wireless safety/security seal that if broken an alarm will be triggered, the status (0/1) of which can be read by an RFID reader from a unique address in its EPC register. Figure 1 shows the pin configuration for the G2IL+, where RFP/RFN is the antenna input port and a switch/link connecting VDD and OUT provides the tamper loop function. The antenna input impedance at the European RFID band of 866MHz is $Z_{chip} = 25 - j237\Omega$ and the passive chip sensitivity is -18dBm.

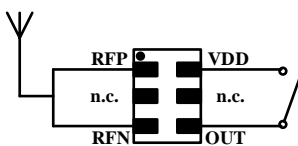


Figure 1: Pin configuration for the G2IL+.

RFID devices may be paralleled and share the same antenna providing appropriate matching is applied. Paralleling eight G2IL+ devices to a single antenna results in eight switchable inputs which when binary weighted yields a tag with an 8-bit counter offering a code range of 0-255. A block diagram is shown in Figure 2.

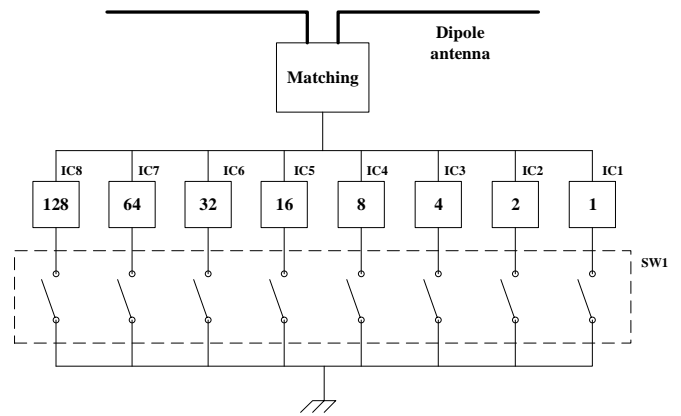
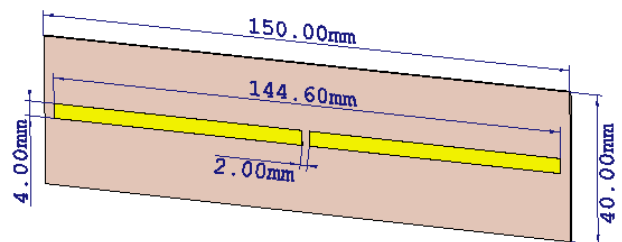


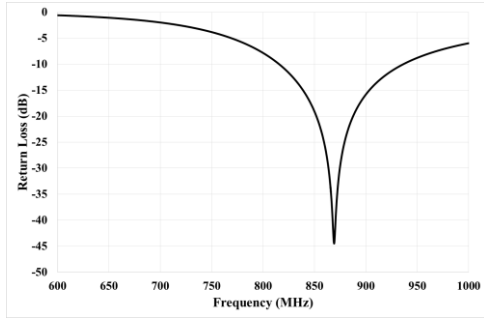
Figure 2: Block diagram of a single antenna 8-bit UHF RFID tag.

3 Tag design

Using CST MWS™ a simple dipole was selected and designed for the European RFID band of 866MHz. Impedance matching was not included as part of the antenna design as lumped element components were used to match the resonant dipole real impedance to the complex impedance of the eight paralleled devices. The dipole is on a 0.8mm FR4 ($\epsilon_r = 4.3$) substrate, as is the rest of the circuitry. The dipole dimensions are shown in Figure 3(a) and its return loss in Figure 3(b) for a 62 Ω port impedance.



(a)

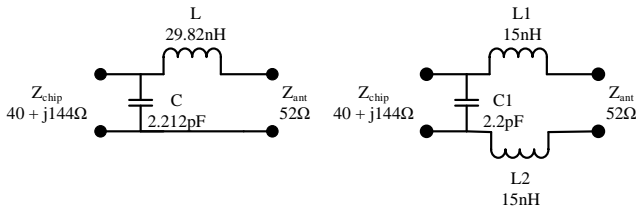


(b)

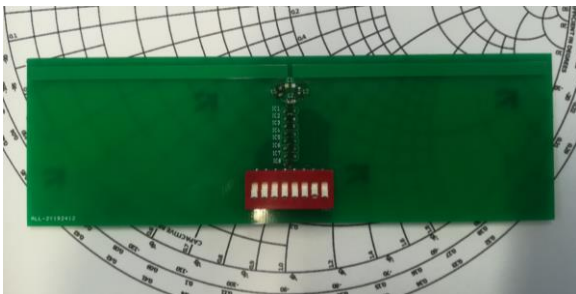
Figure 3: Prototype tag dimensions in (a) and its simulated return-loss in (b).

2.1 Antenna to device impedance matching

The G2IL+ devices are paralleled in a column format keeping PCB tracks as short as practically possible with the input switching mounted below them. With the PCB designed and fabricated - minus the matching components - VNA measurements of both the antenna and the eight paralleled devices were taken at 866MHz. This gave impedances of 52Ω for the antenna and $40 + j144 \Omega$ for the RFID devices. Knowing these values a differential match was calculated by dividing L-match calculated inductance by two and applying the result to both halves of the antenna port as shown in Figure 4 (a). The calculated values are $L1/L2 = 14.91 \text{ nH}$ and $C1 = 2.212 \text{ pF}$. Nearest preferred values (NPV) of 15 nH and 2.2 pF were used. The constructed test tag is shown in Fig. 4 (b). The input stimulus for each device is provided by an 8-way dual in-line package (DIP) switch.



(a)



(b)

Figure 4: L-match to differential match transformation shown in (a). Constructed prototype test tag in (b).

4 Practical RF measurements

With the prototype tag constructed and matched an initial read range measurement was carried out using the Voyantic Tagformance UHF RFID measuring system. This resulted in a read range distance of $\sim 5.5 \text{ m}$ as shown in Fig. 5. Secondly, RSSI measurements were taken over several distances from the reader, this was to determine if all paralleled devices are performing equally. The results of which are shown in Table 1.

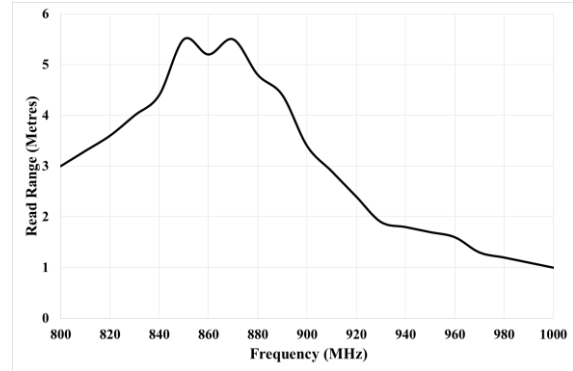


Figure 5: Voyantic read-range measurement of $\sim 5.5 \text{ m}$ for the experimental tag.

	RSSI (dBm)								
	IC1 (0001)	IC2 (0002)	IC3 (0004)	IC4 (0008)	IC5 (0016)	IC6 (0032)	IC7 (0064)	IC8 (0128)	
Read Distance (Meters)	1	-52	-46	-53	-49	-50	-47	-52	-45
	2	-58	-50	-57	-52	-54	-50	-57	-50
	4	-66	-54	-62	-57	-59	-54	-62	-55

Table 1: RSSI measurements for all devices over a range of distances from the reader antenna.

5 Reader side software implementation

In order to facilitate the capture and analysis of the NXP G2IL+ tamper proof switch status, a software application was devised to interrogate the chip and provide a graphical output of its status. The software utilised the Octane SDK provided by Impinj [7] allowing for direct communication to the Impinj R220 Reader. The reader was setup with a custom IP to allow communications through Ethernet. The rest of the primary settings for the reader were left at the default for the EU region.

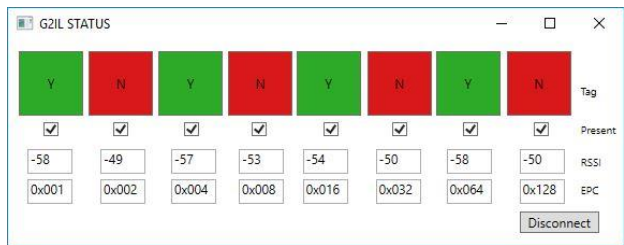
Within this test, the EPC's of the G2IL+ chips had been predefined as $\{ "0001", "0002", "0004", "0008", "0016", "0032", "0064", "0128" \}$ and were individually selectable through DIP switches on the tag. With these values, each of the GUI elements could be assigned to the corresponding G2IL+ chip. This meant that the dip switches corresponded with the correct GUI elements, showing a clear toggle between green and red when the switch was moved between its two states of high and low. The software shows if the specific GUI elements associated with the tag are within the read field,

along with the signal strength, thus allowing the user to diagnose any stuck switches.

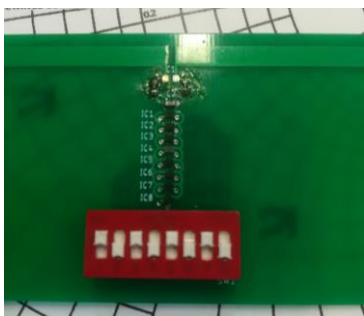
To obtain the status of the tamperproof bit within the G2IL+ chip, all tags that responded to the initial scan are interrogated with a pre-defined read request of the EPC memory bank at 0x200 for a single word. A single word is read due to this being the minimum data size allowed by the Octane SDK. The outcome of this read determines whether the tamperproof loop has been broken or not, returning 0x8040 when the loop is broken and 0x0040 when the loop is intact. Once the status of the loop is obtained, the GUI can be updated accordingly. If corruption occurs in the data transfer the software will default to a tamper intact status until a new tamper register value is received.

The implementation of the software allows for the status bit of each EPC of a G2IL+ tag to be further assigned to other metrics such as using the input to designate a counter. This could be achieved by using the bitwise EPC as its value to create a basic binary counter.

The system in its current form will allow for more chips to be added to system, with the only requirement being that their EPC's be added to the primary EPC array list. The software will generate a suitable number of GUI elements based on the expected number of tags in the array list. The Octane SDK had no problems dealing with the eight-tag design, and it is anticipated that it could handle more chips.



(a)



(b)

Figure 6: G2IL+ Software Analysis Graphical User Interface in (a) Associated dip switch configuration in (b).

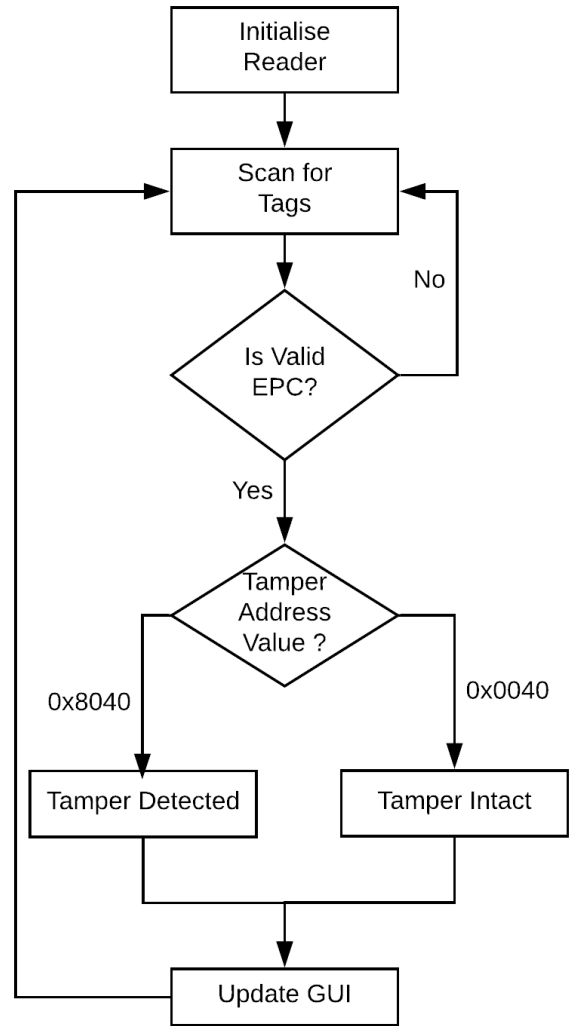


Figure 7: G2IL+ Software Analysis algorithm flow chart.

6 Conclusions

A method of achieving a multi digital input RFID tag has been shown. Here an 8-bit version has been prototyped, the same technique would work for applications of less than 8-bits but the maximum upper limit of paralleled devices is yet to be determined from an RF point of view. The read range is considered reasonable but less than that of a single G2IL+ device. This is mainly due to impedance variations of the PCB layout. Differences in each device input impedance and read sensitivity may also be a contributing factor.

Further research is being conducted into parameterising the performance of the G2IL+ chips in regards to the maximum data rate than be achieved through this passive methodology. Utilising a toggle signal into each of the G2IL+ loops will enable the maximum toggle frequency and data integrity rate. This can be achieved by attaching a cypress PSOC and creating a toggling digital fabric.

The technique presented here is a proof-of-concept with switches providing the input stimulus, simply changing those switches for a switched gray or binary code encoder a passive

level or angular displacement measuring sensor is realised. They could be applied for passive counting applications such as RFID based dosage monitoring of asthma inhalers.

Acknowledgements

This research was supported by EPSRC project EP/R02331X/1

References

- [1] M. A. Ziai and J. C. Batchelor, "Tilt and tamper sensing UHF RFID security tag," *Loughborough Antennas & Propagation Conference (LAPC 2017)*, Loughborough, 2017, pp. 1-5.
doi: 10.1049/cp.2017.0257
- [2] M. A. Ziai and J. C. Batchelor, "Multi-State Logging Freeze Detection Passive RFID Tags," in *IEEE Transactions on Antennas and Propagation*, vol. 62, no. 12, pp. 6406-6411, Dec. 2014.
doi: 10.1109/TAP.2014.2359474
- [2] M. C. Caccami, C. Miozzi, M. Y. S. Mulla, C. Di Natale and G. Marrocco, "An epidermal graphene oxide-based RFID sensor for the wireless analysis of human breath," *2017 IEEE International Conference on RFID Technology & Application (RFID-TA)*, Warsaw, 2017, pp. 191-195.
doi: 10.1109/RFID-TA.2017.8098641
- [3] C. Occhiuzzi and G. Marrocco, "Constrained-Design of Passive UHF RFID Sensor Antennas," in *IEEE Transactions on Antennas and Propagation*, vol. 61, no. 6, pp. 2972-2980, June 2013.
doi: 10.1109/TAP.2013.2250473
- [4] J. C. Batchelor, O. O. Rakibet, C. V. Rumens and S. J. Holder, "Skin-mounted RFID sensing tattoos for assistive technologies," *2014 IEEE MTT-S International Microwave Workshop Series on RF and Wireless Technologies for Biomedical and Healthcare Applications (IMWS-Bio2014)*, London, 2014, pp. 1-3.
doi: 10.1109/IMWS-BIO.2014.7032434
- [5] R. Colella and L. Catarinucci, "Electromagnetic Design of UHF RFID Tags Enabling a Novel Method to Retrieve Sensor Data," in *IEEE Journal of Radio Frequency Identification*, vol. 2, no. 1, pp. 23-30, March 2018.
doi: 10.1109/JRFID.2018.2822689
- [6] https://www.nxp.com/docs/en/data-sheet/SL3S1203_1213.pdf (online) accessed 23/07/2018
- [7] Impinj Octane <https://support.impinj.com/hc/en-us/articles/202755268-Octane-SDK> (online) accessed 23/07/2018